

A Stabilized and Coupled Meshfree/Meshbased Method for the Incompressible Navier-Stokes Equations — Part II: Coupling

Thomas-Peter Fries, Hermann G. Matthies
Institute of Scientific Computing
Technical University Braunschweig
Brunswick, Germany

Informatikbericht Nr.: 2005-03

February, 2005



A Stabilized and Coupled Meshfree/Meshbased Method for the Incompressible Navier-Stokes Equations — Part II: Coupling

Thomas-Peter Fries, Hermann G. Matthies
Department of Mathematics and Computer Science
Technical University Braunschweig
Brunswick, Germany

February, 2005

Location

Institute of Scientific Computing
Technical University Braunschweig
Hans-Sommer-Strasse 65
D-38106 Braunschweig

Postal Address

Institut für Wissenschaftliches Rechnen
Technische Universität Braunschweig
D-38092 Braunschweig
Germany

Contact

Phone: +49-(0)531-391-3000
Fax: +49-(0)531-391-3003
E-Mail: wire@tu-bs.de
www: <http://www.tu-bs.de/institute/WiR>

Copyright © by Institut für Wissenschaftliches Rechnen, Technische Universität Braunschweig

This work is subject to copyright. All rights are reserved, whether the whole or part of the material is concerned, specifically the rights of translation, reprinting, reuse of illustrations, recitation, broadcasting, reproduction on microfilm or in any other way, and storage in data banks. Duplication of this publication or parts thereof is permitted in connection with reviews or scholarly analysis. Permission for use must always be obtained from the copyright holder.

Alle Rechte vorbehalten, auch das des auszugsweisen Nachdrucks, der auszugsweisen oder vollständigen Wiedergabe (Photographie, Mikroskopie), der Speicherung in Datenverarbeitungsanlagen und das der Übersetzung.

A Stabilized and Coupled Meshfree/Meshbased Method for the Incompressible Navier-Stokes Equations — Part II: Coupling

Thomas-Peter Fries, Hermann G. Matthies

February, 2005

Abstract

In part I of this work, meshfree Galerkin methods have been used for the approximation of the incompressible Navier-Stokes equations in Eulerian or arbitrary Lagrangian-Eulerian formulation. The problem of stabilization of meshfree methods is addressed there. Analogously, in the meshbased context, the finite element method is frequently used in similar stabilized formulations for the simulation of flow problems. In order to combine the advantages of both methods, different coupling techniques are examined in this part of the work. Standard coupling approaches are modified in order to fulfill the requirements for a reliable stabilization found in part I of this work. The resulting stabilized and coupled meshfree/meshbased flow solver employs the comparatively costly meshfree Galerkin method only where it is needed—i.e. in areas of the domain, where a mesh is difficult to maintain—, and the efficient meshbased finite element method in the rest of the domain. This enables the solution of complex flow problems, as thus involving large deformations of the physical domain and/or moving and rotating obstacles.

Contents

1	Introduction	3
2	Meshbased and Meshfree Shape Functions	4
3	Governing Equations	5
4	Coupling	7
4.1	Preliminaries	8
4.2	Coupling with Consistency Conditions	8
4.3	Coupling with a Ramp Function	10
5	Numerical results	12
5.1	One-dimensional Advection-Diffusion Equation	12
5.2	Incompressible Navier-Stokes Equations	14
5.2.1	Driven Cavity Flow	14
5.2.2	Cylinder Flow	14
5.2.3	Flow around a Rotating Obstacle	16
6	Conclusion	17
	References	19

1 Introduction

Stabilized meshbased methods have developed to be standard tools for the simulation of flow problems [9, 21, 22, 50], they enable efficient and reliable approximations of the differential equations in fluid flow. However, in certain applications, for example in the presence of large geometric deformations of the boundary or rotating and moving obstacles—situations which may frequently occur in the context of fluid-structure interaction problems—, the maintenance of a conforming mesh may be almost impossible. Different elaborate techniques have been developed to deal with these problems in the meshbased context: the fictitious domain [5, 20] and fictitious boundary methods [47], techniques employing overlapping grids [8, 23, 43, 49]—also called Chimera methods—, sliding mesh techniques [1, 2], level-set methods [40], or standard arbitrary Lagrangian-Eulerian (ALE) formulations with frequent remeshing [36].

A different way to handle complex flow problems is to employ a comparably new and innovative class of methods, which enables the approximation of partial differential equations based on a set of nodes, without the need for an additional mesh. These meshfree methods (MMs) [3, 13] are generally able to solve problems where meshes bring up difficulties. However, these methods are comparably time-consuming, especially in Galerkin settings, which limits their usefulness in the simulation of challenging real-life problems.

Therefore, we *couple* meshfree and meshbased methods in order to use meshfree methods only in small parts of the domain, where they are needed because a mesh may be particularly difficult to be maintained there, and use standard meshbased methods in the rest of the domain. For this purpose several coupling approaches have been proposed e.g. in [4, 24, 35]. The coupling approach of Belytschko *et al.* [4] employs ramp functions for the blending of the meshfree and meshbased parts of the domain. It is restricted to first order consistency, very similar versions of this approach are found in [7, 32]. The approach of Huerta *et al.* [24] considers the contribution of the finite element shape functions in the computation of the meshfree shape functions. Also higher-order coupled shape functions may be obtained with this technique. The bridging scale method of Liu *et al.* [35] may also be used to couple meshfree and meshbased shape functions. However, this approach requires meshfree and meshbased shape functions everywhere in the computational domain, thereby not reducing the computational effort of the coupled formulation. Hence, it is not considered here.

Coupling meshfree and meshbased methods has also been performed with the aim to combine other advantages of both methods. It may be desirable to introduce the favorable characteristics of meshfree methods with respect to continuity [31, 33], adaptivity [12], enrichment [28, 29] etc. Methods like the Generalized Finite Element Method [44, 45], Partition of Unity Finite Element Method [37] and *hp*-clouds [10, 11, 39] may also be considered as hybrids of meshfree and meshbased methods, as they combine ideas from both areas.

For both, the meshbased and meshfree parts of the domain the weak form of the incompressible Navier-Stokes equations in Eulerian or ALE formulation [27] are approximated. This is standard for meshbased methods—where it would be almost impossible to take the Lagrangian viewpoint and maintain a conforming mesh throughout the flow simulation—and is also applied for the meshfree part in order to make the coupling as straightforward as possible. The Eulerian and ALE viewpoint requires stabilization, which is discussed in detail in part I of this work [18], see

also [15, 17]. There, it has been shown that standard stabilization methods may be applied to meshfree methods as well, however, with a careful choice of the stabilization parameter τ which weighs the stabilization. Only small dilatation parameters of the meshfree shape functions justify the use of standard formulas for τ .

In the context of coupled meshfree/meshbased shape functions it is found that the standard coupling approaches of [4, 24] require modifications, see also [14, 16]. The approach of Huerta *et al.* [24] is modified in a way that smaller dilatation parameters of the meshfree shape functions are possible, being more suitable for stabilization. The approach of Belytschko *et al.* [4] is modified slightly such that the shape functions are more regular in the transition area where meshfree and meshbased functions are coupled, which is also advantageous for stabilization. The resulting stabilized and coupled formulation is validated and successfully applied to a number of test cases.

The plan of the paper is as follows: In section 2 the meshfree and meshbased shape functions are defined. Standard bi-linear finite element shape functions and moving least-squares (MLS) shape functions are employed. The next section describes the governing equations of incompressible, instationary flows in strong and SUPG/PSPG-stabilized weak form. Section 4 starts with a review of various coupling approaches with different emphases. Then, the approaches of [4] and [24] are described. The modifications in order to obtain coupled shape functions that are more suitable for stabilization are introduced. In section 5 the success of the stabilized and coupled formulation is shown starting with a convergence test of the one-dimensional advection-diffusion equation using the different coupling approaches. Then, the coupled formulations are applied to the incompressible Navier-Stokes equations. The fluid solver is validated with two standard test cases, and applied to a problem involving a moving and rotating object. All test cases show that the coupled approximations have the same order of convergence as pure FEM calculations, and that reliable and accurate solutions are obtained with the modified coupling approaches. Section 6 ends this paper with some conclusion.

2 Meshbased and Meshfree Shape Functions

FEM approximations may be written in the following form

$$u^h(\mathbf{x}) = \sum_{i \in I^{\text{FEM}}} N_i^{\text{FEM}}(\mathbf{x}) u_i = (\mathbf{N}^{\text{FEM}}(\mathbf{x}))^T \mathbf{u}, \quad (2.1)$$

where $\mathbf{N}^{\text{FEM}}(\mathbf{x})$ are the finite element shape functions of the nodes in I^{FEM} . The shape function of a node consists of contributions of element shape functions in the surrounding elements of that node, therefore, it is often convenient to define shape functions element-wise. The element-wise interpolation in an iso-parametric element is [26]

$$u_i^h(\mathbf{x}) = \sum_{I=1}^{n_{\text{en}}} N_I^{\text{FEM,el}}(\mathbf{x}) u_{iI}, \quad (2.2)$$

where n_{en} is the number of nodes per element. The functions $N_I^{\text{FEM,el}}$ are standard bi-linear finite element shape functions [51].

For the meshfree part, the shape function are computed with the MLS technique [30] as briefly

described in part I of this work [18], a detailed discussion may be found in [3, 13]. The MLS approximation is

$$\mathbf{u}^h(\mathbf{x}) = \sum_{i \in I^{\text{MLS}}} N_i^{\text{MLS}}(\mathbf{x}) u_i = (\mathbf{N}^{\text{MLS}}(\mathbf{x}))^T \mathbf{u} \quad (2.3)$$

with

$$(\mathbf{N}^{\text{MLS}}(\mathbf{x}))^T = \mathbf{p}^T(\mathbf{x}) [\mathbf{M}(\mathbf{x})]^{-1} \mathbf{B}(\mathbf{x}), \quad (2.4)$$

$$\mathbf{M}(\mathbf{x}) = \sum_{i \in I^{\text{MLS}}} w(\mathbf{x} - \mathbf{x}_i) \mathbf{p}(\mathbf{x}_i) \mathbf{p}^T(\mathbf{x}_i), \quad (2.5)$$

$$\mathbf{B}(\mathbf{x}) = \begin{bmatrix} w(\mathbf{x} - \mathbf{x}_1) \mathbf{p}(\mathbf{x}_1) & \dots & w(\mathbf{x} - \mathbf{x}_n) \mathbf{p}(\mathbf{x}_n) \end{bmatrix}, \quad (2.6)$$

where \mathbf{N}^{MLS} are the meshfree shape functions corresponding to the nodes in the set I^{MLS} . $w(\mathbf{x} - \mathbf{x}_i)$ is a Gaussian like weighting function which is defined on small supports $\tilde{\Omega}_i$ around each node. These supports are defined by the *dilatation parameter* ρ_i and define directly the support of the resulting MLS functions. $\mathbf{p}(\mathbf{x})$ is a complete polynomial basis and depends on the dimension and the desired consistency of the MLS functions. Throughout this paper linear consistency is considered in two dimensions, hence $\mathbf{p}(\mathbf{x}) = [1, x, y]$. This enables the MLS functions employed as shape functions in a Galerkin weak form to find linear solutions exactly.

3 Governing Equations

The instationary, incompressible Navier-Stokes equations are considered in velocity-pressure formulation. Let Ω and $(0, T)$ be the spatial and temporal domain, then

$$\varrho \left(\frac{\partial \mathbf{u}}{\partial t} + \mathbf{u} \cdot \nabla \mathbf{u} - \mathbf{f} \right) - \nabla \cdot \boldsymbol{\sigma} = 0, \quad \text{on } \Omega \times (0, T) \quad (3.1)$$

$$\nabla \cdot \mathbf{u} = 0, \quad \text{on } \Omega \times (0, T), \quad (3.2)$$

where \mathbf{u} are the velocities and ϱ is the density. The stress tensor $\boldsymbol{\sigma}$ is defined as

$$\boldsymbol{\sigma} = -p\mathbf{I} + 2\mu\boldsymbol{\varepsilon}(\mathbf{u}), \quad \text{with } \boldsymbol{\varepsilon}(\mathbf{u}) = \frac{1}{2} \left(\nabla \mathbf{u} + (\nabla \mathbf{u})^T \right),$$

where p is the pressure and μ the dynamic viscosity. The initial condition is given as $\mathbf{u}_0 = \mathbf{u}(\mathbf{x}, 0)$, $\nabla \cdot \mathbf{u}_0 = 0$, and the Dirichlet and Neumann boundary conditions are applied along complementary subsets of the boundary of Ω , Γ_g and Γ_h , as

$$\mathbf{u} = \mathbf{g} \quad \text{on } \Gamma_g, \quad (3.3)$$

$$\boldsymbol{\sigma} \cdot \mathbf{n} = \mathbf{h} \quad \text{on } \Gamma_h. \quad (3.4)$$

The test and trial functions for the velocities and pressure are from the sets

$$\mathcal{S}_{\mathbf{u}}^h = \left\{ \mathbf{u}^h \mid \mathbf{u}^h \in (\mathcal{H}^{1h})^{n_d}, \mathbf{u}^h = \mathbf{g}^h \text{ on } \Gamma_g \right\}, \quad (3.5)$$

$$\mathcal{V}_{\mathbf{u}}^h = \left\{ \mathbf{w}^h \mid \mathbf{w}^h \in (\mathcal{H}^{1h})^{n_d}, \mathbf{w}^h = 0 \text{ on } \Gamma_g \right\}, \quad (3.6)$$

$$\mathcal{S}_p^h = \mathcal{V}_p^h = \left\{ q^h \mid q^h \in \mathcal{H}^{1h} \right\}, \quad (3.7)$$

where n_d is the number of space dimensions and \mathcal{H}^{1h} is a finite dimensional space built by the set of shape functions. Time integration is performed with a Crank-Nicholson scheme, see e.g. [9].

According to part I of this work [18], the meshbased FEM and meshfree MLS functions are applied to the SUPG/PSPG stabilized weak form of the incompressible Navier-Stokes equations in two dimensions. The GLS-stabilization is not considered because in part I it turned out that this formulation leads to slightly more diffusive results. The approximation of the weak form of the SUPG/PSPG stabilized incompressible Navier-Stokes equations in ALE formulation may be stated as follows [46]: find $\mathbf{u}^h \in \mathcal{S}_u^h$ and $p^h \in \mathcal{S}_p^h$ such that

$$\begin{aligned}
& \int_{\Omega} \mathbf{w}^h \cdot \varrho \left(\frac{\partial \mathbf{u}^h}{\partial t} + \bar{\mathbf{u}}^h \cdot \nabla \mathbf{u}^h - \mathbf{f}^h \right) d\Omega + \int_{\Omega} \boldsymbol{\varepsilon}(\mathbf{w}^h) : \boldsymbol{\sigma}^h(\mathbf{u}^h, p^h) d\Omega + \int_{\Omega} q^h \nabla \cdot \mathbf{u}^h d\Omega \\
& + \sum_{e=1}^{n_{el}} \int_{\Omega_e} \tau \left(\bar{\mathbf{u}}^h \cdot \nabla \mathbf{w}^h + \frac{1}{\varrho} \nabla q^h \right) \cdot \left[\varrho \left(\frac{\partial \mathbf{u}^h}{\partial t} + \bar{\mathbf{u}}^h \cdot \nabla \mathbf{u}^h - \mathbf{f}^h \right) - \nabla \cdot \boldsymbol{\sigma}^h(\mathbf{u}^h, p^h) \right] d\Omega \\
& = \oint_{\Gamma_h} \mathbf{w}^h \cdot \mathbf{h}^h d\Gamma \quad \forall \mathbf{w}^h \in \mathcal{V}_u^h, \forall q^h \in \mathcal{V}_p^h.
\end{aligned} \tag{3.8}$$

According to the ALE technique [27], the advection velocity \mathbf{u} is changed to $\bar{\mathbf{u}} = \mathbf{u} - \boldsymbol{\chi}$, where $\boldsymbol{\chi}$ is the mesh velocity.

It is important to note that the meshbased bi-linear finite element shape functions are only C^0 -continuous in Ω . However, stabilization terms introduce second order derivatives, therefore, the stabilization influence is considered in element interiors only ($\sum \int_{\Omega_e}$). It may be shown that this restriction influences the consistency of the formulation (e.g. stabilized diffusion terms are largely under-represented [6]), eventually degrading the order of convergence in certain applications [25]. In contrast, meshfree shape functions may easily be constructed to have any desired order of continuity and second derivatives are well defined everywhere in Ω . Then, the expression $\sum \int_{\Omega_e}$ may simply be replaced by \int_{Ω} .

The second line of (3.8) represents the stabilization. It consists of perturbation terms multiplied with residual forms, weighted by the stabilization parameter τ . The choice of suitable τ is a crucial aspect for the success of a stabilization [42]. In part I of this work [18] it is discussed in detail which formulas for τ may be used in a meshfree context. It is found that only for small dilatation parameters of the meshfree shape functions standard formulas for τ , derived in a meshbased context, are suitable. Herein, the following formula for τ [42] is used for the purely meshbased and meshfree shape functions, as well as for the coupled shape functions:

$$\tau = 1 \left/ \sqrt{\left(\frac{2}{\Delta t}\right)^2 + \left(\frac{2\|\mathbf{u}^h\|}{h}\right)^2 + \left(\frac{4\nu}{h^2}\right)^2} \right. . \tag{3.9}$$

There is a close similarity to the coth-formula used for the stabilization of the stationary Navier-Stokes equations in part I, see also [15]. The parameter h is a measure of the support of a shape function. It is either the element length h_e for the meshbased shape functions or the support length h_ρ for the meshfree shape functions. For suitable choices of h_e see e.g. [38], and for h_ρ see part I of this work [18].

4 Coupling

Coupling meshfree and meshbased methods has been realized in many different ways. The aim is always to combine certain advantages of each method. We find the following examples:

Continuity: Meshfree shape functions may be constructed to have any desired order of continuity, see e.g. [13]. In contrast, meshbased shape functions are often only C^0 -continuous in the domain. The construction of higher-order continuous finite element shape functions in multi-dimensions poses serious problems, see e.g. [31]. With the aim to construct element shape functions with any desired order of continuity, Li, Liu *et al.* introduce the Reproducing Kernel Element Method, see [33] and [31].

Adaptivity: The absence of a mesh in meshfree methods is advantageous for adaptive strategies. Only nodes have to be added or removed where desired, without the need to keep a conforming mesh. In [12], Fernández *et al.* make use of this fact and introduce meshfree areas in a FEM domain where adaptivity is desired.

Enrichment: The enrichment of the approximation space with certain functions may drastically improve the convergence properties of a numerical method. This is comparably easy possible with some meshfree methods such as the generalized finite element method (GFEM) [44, 45], partition of unity finite element method (PUFEM) [37] and *hp*-clouds [10, 11, 39]. These methods combine ideas from the FEM and MMs. More direct approaches for coupling meshfree and meshbased methods for enrichment may be found in [24, 35].

Meshing: In problems involving large geometry deformations, moving boundaries, or moving and rotating objects, maintaining of a conforming mesh is often very difficult. Furthermore, the costs for frequent remeshing—which may even fail in complex geometric situations—are not negligible, and projection errors between the meshes are introduced [28]. Thus, it may be desirable to employ meshfree shape functions in parts of the domain, where a mesh causes problems, and meshbased shape functions in the remaining area. Coupling approaches for meshbased and meshfree shape functions may be found in Belytschko *et al.* [4], in Huerta *et al.* [24], and in Liu *et al.* [35, 48]. Other ways are shown in [28, 29]. The meshing aspect is closely related to connectivity: Sometimes the connectivity of the nodes in parts of the domain changes during runtime (e.g. in case of a rotating object), then it may be desirable to use meshfree shape functions there, because they compute the connectivity at run-time, in contrast to meshbased methods which define the connectivity *a priori* with a mesh.

Computational effort: Meshfree shape functions are comparably expensive to compute. The functions are of a highly non-polynomial character, which makes integration in a Galerkin setting demanding. Large numbers of integration points are necessary, and at each integration point a small system of equations ($\mathbf{M}(\mathbf{x})$) has to be built up—including a neighbour search—and inverted in order to determine the meshfree shape functions. The computation of the shape functions' derivatives involves matrix-vector operations whose costs are not negligible. Therefore, it is often desirable from a computational viewpoint to use meshfree shape functions as little as possible. Consequently, the aim is to employ meshfree shape func-

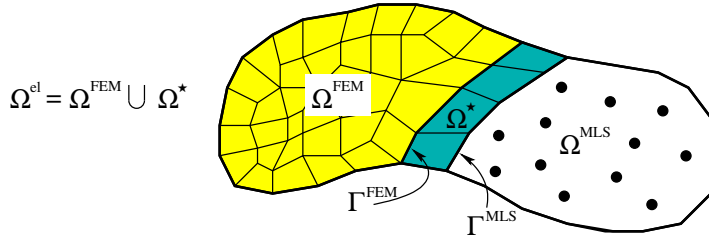


Figure 1: Decomposition of the domain into Ω^{FEM} , Ω^{MLS} and Ω^* .

tions where their properties are desirable—according to any of the previous aspects—and meshbased shape function in the rest of the domain.

Here, the aim is to develop a coupled meshfree/meshbased fluid solver which is able to simulate complex flow phenomena including large geometry deformations and moving and rotating obstacles. Therefore, the meshing aspect together with the consideration of the computational effort is important. Thus, the approaches of Belytschko *et al.* [4] and Huerta *et al.* [24] for coupling meshbased and meshfree shape functions may be chosen. The approach in [4] employs ramp functions in the transition area between the purely meshfree and meshbased parts of the domain, whereas the approach in [24] modifies the consistency conditions of the MLS procedure considering the contributions of the finite element shape functions in the transition area. We do not consider the approach of [35, 48] (bridging scale method), as there—due to continuity requirements—the coupling may only be performed for meshfree and meshbased shape functions defined everywhere in the domain, not leading to reduced computational cost.

4.1 Preliminaries

For a coupling of meshfree and meshbased shape functions, the domain Ω is decomposed into disjoint domains Ω^{el} and Ω^{MLS} , with the common boundary Γ^{MLS} . The domain Ω^{el} is discretized with standard quadrilateral finite elements. The union of all elements along Γ^{MLS} is called the transition area Ω^* , so that Ω^{el} may further be decomposed into the disjoint domains Ω^{FEM} and Ω^* , connected by a boundary labeled Γ^{FEM} ; clearly $\Omega^{\text{FEM}} \cap \Omega^{\text{MLS}} = \emptyset$. This situation is sketched in Fig. 1.

Throughout this paper, consistency of first order is fulfilled by the set of meshbased, meshfree and coupled shape functions. This results in the ability of reproducing linear solutions *exactly*.

4.2 Coupling with Consistency Conditions

The coupling approach of Huerta *et al.* [24] considers the contributions of the meshbased FEM shape functions in the computation of the MLS shape functions by modified consistency conditions; see [13] for an alternative deduction of this coupling approach. The resulting coupled set of shape functions is consistent up to the desired order.

In the original approach [24], FEM nodes are placed in the standard way in the elements inside Ω^{FEM} , however *not* in $\Omega^* \setminus \Gamma^{\text{FEM}}$. The corresponding meshbased shape functions of the FEM nodes *remain unchanged*, and the coupling is considered only in the meshfree shape functions. Meshfree

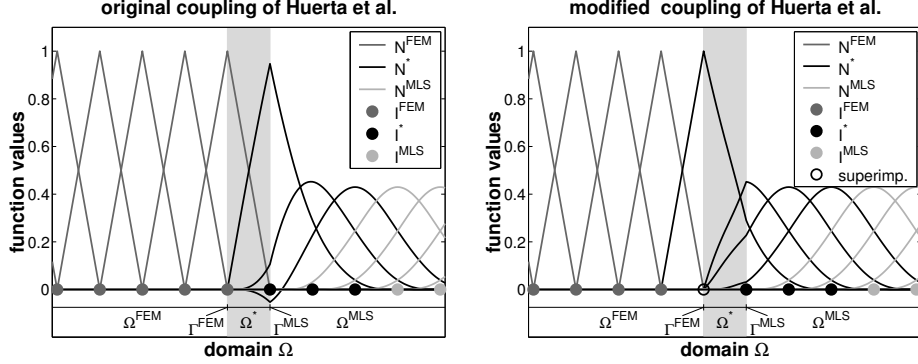


Figure 2: Shape functions of the coupling approach of Huerta in the original [24] and modified version.

nodes with corresponding supports $\tilde{\Omega}_i$ may be arbitrarily distributed in Ω^{MLS} and Ω^* . Then, the meshbased and meshfree shape functions for the nodes are computed as follows:

$$\begin{aligned}
 \text{FEM: } N_i &= N_i^{\text{FEM}} & \forall i \in I^{\text{FEM}}, \\
 \text{MLS: } N_i &= N_i^{\text{MLS}} & \forall i \in I^{\text{MLS}}, \\
 \text{coupled: } N_i &= \begin{pmatrix} \mathbf{p}^T(\mathbf{x}) - \sum_{j \in I^{\text{FEM}}} N_j^{\text{FEM}}(\mathbf{x}) \mathbf{p}^T(\mathbf{x}_j) \\ [\mathbf{M}(\mathbf{x})]^{-1} w(\mathbf{x} - \mathbf{x}_i) \mathbf{p}(\mathbf{x}_i) \end{pmatrix} & \forall i \in I^*,
 \end{aligned} \tag{4.1}$$

with

$$I^{\text{FEM}} = \{i \mid \mathbf{x}_i \in \Omega^{\text{FEM}}\}, \tag{4.2}$$

$$I^{\text{MLS}} = \{i \mid \tilde{\Omega}_i \subset \Omega^{\text{MLS}}\}, \tag{4.3}$$

$$I^* = \{i \mid \tilde{\Omega}_i \cap \Omega^{\text{el}} \neq \emptyset\}. \tag{4.4}$$

In words, I^{MLS} is the set of meshfree nodes whose supports are fully inside Ω^{MLS} , and I^* is the set of MLS nodes that have supports overlapping with elements. N_i^{FEM} are the standard bi-linear finite element shape functions, and N_i^{MLS} are the standard MLS functions, defined in section 2. Fig. 2 shows the sets I^{FEM} , I^{MLS} and I^* and displays the resulting shape functions of this approach in a section of a one-dimensional domain with a regular node distribution around the transition area Ω^* .

Modification Instead of keeping the FEM shape function unchanged inside the transition area as in the original approach, one may additionally place meshfree nodes at the FEM node positions along Γ^{FEM} and superimpose the two shape functions at these nodes. That is, I^{FEM} reduces to $\{i \mid \mathbf{x}_i \in \Omega^{\text{FEM}} \setminus \Gamma^{\text{FEM}}\}$, and for the nodes along Γ^{FEM} we define

$$\text{coupled: } N_i = \begin{pmatrix} \mathbf{p}^T(\mathbf{x}) - \sum_{j \in I^{\text{FEM}}} N_j^{\text{FEM}}(\mathbf{x}) \mathbf{p}^T(\mathbf{x}_j) \\ [\mathbf{M}(\mathbf{x})]^{-1} w(\mathbf{x} - \mathbf{x}_i) \mathbf{p}(\mathbf{x}_i) + N_i^{\text{FEM}} \end{pmatrix} \quad \forall i : \mathbf{x}_i \in \Gamma^{\text{FEM}}. \tag{4.5}$$

The right part of Fig. 2 shows the resulting shape functions of the modified approach of [24].

The important advantage of this modification is that smaller dilatation parameters are possible (although in this figure $\rho_i = 2.9\Delta x$ has been taken for both approaches). For example, in the original approach and a regular distribution of nodes in one dimension, one finds that in case of *linear* consistency for the regularity of the matrix $\mathbf{M}(\mathbf{x})$, dilatation parameters of $\rho_i > 2.0\Delta x$ are required [24]. This follows from the requirement for the regularity of $\mathbf{M}(\mathbf{x})$ [24, 34] that

$$\text{card} \{ \mathbf{x}_j | w(\mathbf{x} - \mathbf{x}_j) \neq 0 \forall j \in I' \} \geq k = \dim(\mathbf{M}), \quad (4.6)$$

with $I' = I^{\text{MLS}} \cup I^*$, which near the boundary Γ^{FEM} can only be fulfilled with $\rho_i > 2.0\Delta x$. In contrast, with the modified approach the nodes along Γ^{FEM} are added to I' , hence $I' = I^{\text{MLS}} \cup I^* \cup \{i | \mathbf{x}_i \in \Gamma^{\text{FEM}}\}$, and thus $\rho_i > 1.0\Delta x$ are sufficient for linear consistency. This holds analogously in multi-dimensional domains and is an important advantage for the reliable stabilization of (non-linear) partial differential equations. This has been discussed in detail in part I of this work [18], see also [15, 17].

4.3 Coupling with a Ramp Function

In the approach of Belytschko *et al.* [4], meshfree and meshbased shape functions for the nodes i are computed and defined independently and coupled with help of a ramp function $R(\mathbf{x})$. FEM nodes are placed in Ω^{el} , in contrast to the coupling approach of [24], where they are placed in Ω^{FEM} only. Meshfree nodes with supports $\tilde{\Omega}_i$ are distributed arbitrarily in $\Omega^* \cup \Omega^{\text{MLS}}$ and may also be included inside Ω^{FEM} . The latter will only affect the shape functions inside $\Omega^* \cup \Omega^{\text{MLS}}$, i.e. MLS nodes with $\tilde{\Omega}_i \subset \Omega^{\text{FEM}}$ have no influence at all. Belytschko *et al.* [4] define the ramp function as follows:

$$R(\mathbf{x}) = \begin{cases} 0 & , \mathbf{x} \in \Omega^{\text{FEM}} \\ 1 & , \mathbf{x} \in \Omega^{\text{MLS}} \\ \sum_{i \in I} N_i^{\text{FEM}}(\mathbf{x}) & , \mathbf{x} \in \Omega^*, I = \{i | \mathbf{x}_i \in \Gamma^{\text{MLS}}\}, \end{cases} \quad (4.7)$$

i.e. it varies monotonically between 0 and 1 in Ω^* . The linear consistency of the resulting set of meshbased, meshfree and coupled shape functions is maintained [4].

The shape functions are defined as follows:

$$\begin{aligned} \text{FEM: } N_i &= N_i^{\text{FEM}} & \forall i \in I^{\text{FEM}}, \\ \text{MLS: } N_i &= N_i^{\text{MLS}} & \forall i \in I^{\text{MLS}}, \\ \text{coupled: } N_i &= [1 - R(\mathbf{x})] N_i^{\text{FEM}} + R(\mathbf{x}) N_i^{\text{MLS}} & \forall i \in I^*, \end{aligned} \quad (4.8)$$

with

$$I^{\text{FEM}} = \left\{ i \mid \mathbf{x}_i \in \Omega^{\text{FEM}}, \tilde{\Omega}_i \subset \Omega^{\text{FEM}} \right\}, \quad (4.9)$$

$$I^{\text{MLS}} = \left\{ i \mid \tilde{\Omega}_i \subset \Omega^{\text{MLS}} \right\}, \quad (4.10)$$

$$I^* = \left\{ i \mid \tilde{\Omega}_i \cap \Omega^{\text{el}} \neq \emptyset \right\}. \quad (4.11)$$

The resulting shape functions are shown in the left part of Fig. 3. One may note that meshfree nodes inside Ω^{FEM} have an undesirable influence in $\Omega^* \cup \Omega^{\text{MLS}}$, leading to a numerically awkward

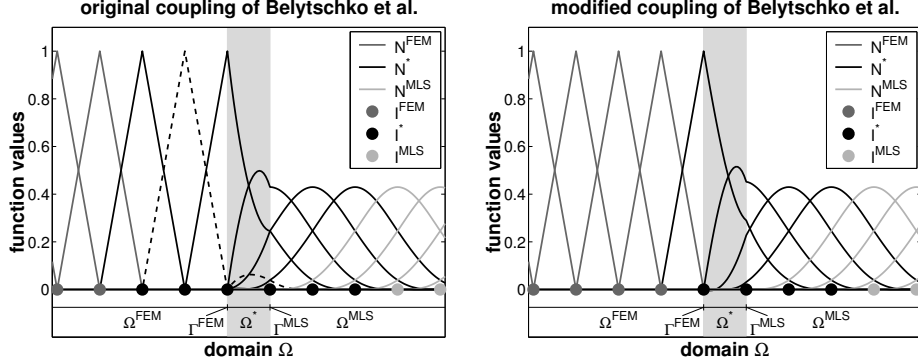


Figure 3: Shape functions of the coupling approach of Belytschko in the original [4] and modified version.

form of the shape function (dashed line in Fig. 3). Especially in the context of stabilization, it is neither clear from a mathematical viewpoint nor from an empirical viewpoint how to choose suitable stabilization parameters for these shape functions, see [15].

Modification In order to avoid these numerically awkward shape functions, this approach is modified slightly. The meshfree nodes are restricted to the area $\Omega^* \cup \Omega^{\text{MLS}}$. The resulting shape functions are then (for sufficiently small dilatation parameters) suitable to motivate the use of standard stabilization parameters [15]. Consequently, a reliable stabilization is obtained. The resulting shape functions of the modified coupling approach of [4] are shown in the right part of Fig. 3.

Fig. 4 compares the sets I^{FEM} , I^{MLS} and I^* in the different versions of the coupling approaches in a two-dimensional domain. It may be seen that the difference between the original approaches from [24] and [4] are that FEM nodes in the former publication are distributed in Ω^{FEM} only, whereas in the latter FEM nodes are in $\Omega^{\text{el}} = \Omega^{\text{FEM}} \cup \Omega^*$. Furthermore, MLS nodes are restricted to $\Omega^{\text{MLS}} \cup \Omega^*$ in the approach in [24], but may be distributed everywhere in Ω in the approach of [4] (however, influence will only be in $\Omega^* \cup \Omega^{\text{MLS}}$). The difference between the modified versions and the original versions are as follows: In the case of the coupling of [24], MLS nodes are also distributed at the FEM nodes along Γ^{FEM} and are superimposed according to (4.5). In the case of the coupling in [4], the MLS nodes are restricted to $\Omega^* \cup \Omega^{\text{MLS}}$ only, because MLS nodes in Ω^{FEM} may show an undesirable influence in $\Omega^* \cup \Omega^{\text{MLS}}$.

Remark 1 In Figs. 2 and 3 it can be seen that the coupled shape functions are only C^0 -continuous along the boundary Γ^{MLS} . It is easily possible to construct shape functions that are C^1 -continuous there and, consequently, restrict C^0 -continuous shape functions to the area Ω^{FEM} . This can be achieved in the approach in [24] by replacing the bi-linear element shape functions in Ω^* by standard Hermitian C^1 -continuous element shape functions [51]. The consistency of the resulting set of coupled shape functions is still ensured due to the modified consistency conditions of this approach. In the coupling approach of [4] C^1 -continuity along Γ^{FEM} can be achieved by using C^1 -continuous ramp functions in Ω^* . Again, Hermitian element shape functions may be used. Fig. 5 shows the resulting C^1 -continuous shape functions and compares them with the C^0 -

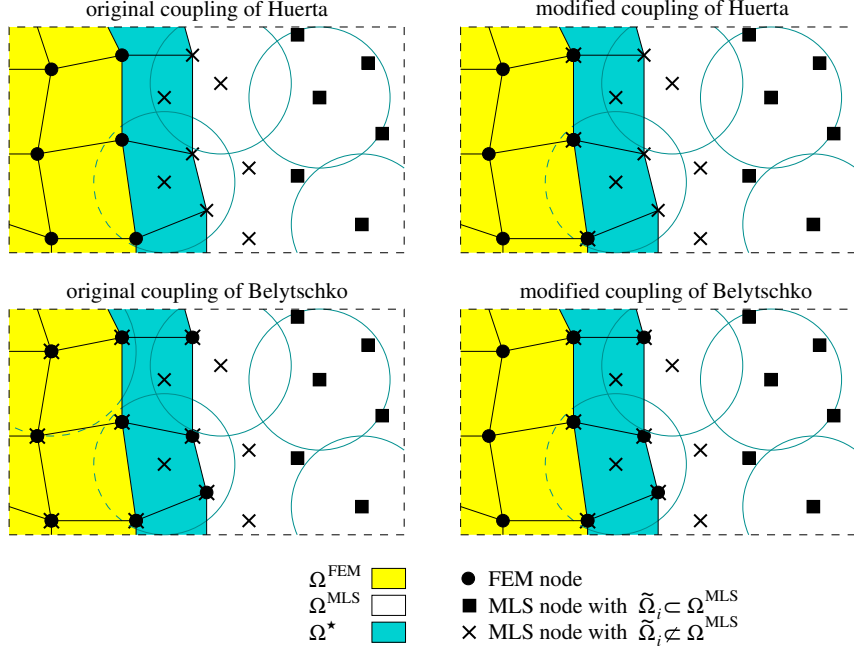


Figure 4: Differences between the sets I^{FEM} , I^{MLS} and I^* in the original and modified coupling versions. The grey circles show the supports $\tilde{\Omega}_i$ of some MLS nodes.

continuous case. Clearly, only the shape functions in Ω^* are effected by the modifications. It is interesting to note that in our own numerical studies the higher order of continuity does not lead to superior results, therefore, throughout this paper only C^0 continuity along Γ^{FEM} is fulfilled by the shape functions.

5 Numerical results

5.1 One-dimensional Advection-Diffusion Equation

The aim of this section is to show that the same order of convergence is obtained with all coupling approaches. The obtained convergence of order 2 in the L_2 -norm is equivalent to purely meshbased computations with linear finite elements only. The test case is defined as follows. The one-dimensional advection-diffusion equation

$$c \frac{\partial u(x)}{\partial x} - K \frac{\partial^2 u(x)}{\partial x^2} = f, \quad x \in (0, 1); \quad c, K \in \mathbb{R} \quad (5.1)$$

in SUPG-stabilized weak form [6] is approximated, with $f = 2c\pi \cos(2\pi x) + 4K\pi^2 \sin(2\pi x)$, $c = 10$, $K = 1$ and boundary conditions $u(0) = u(1) = 0$. The exact solution is $u(x) = \sin(2\pi x)$. Throughout the convergence test, the ratio of the domains is kept constant at $\Omega^{\text{FEM}} : \Omega^* : \Omega^{\text{MLS}} = 6 : 1 : 6$, which may be seen in the left part of Fig. 6. The right part shows the convergence results for the two original and modified coupling approaches of [4] and [24] respectively. The rate of convergence remains the same as in pure FEM computations. As expected, the higher rates of convergence often achieved for a pure MLS approximations are not observed, which is in agreement

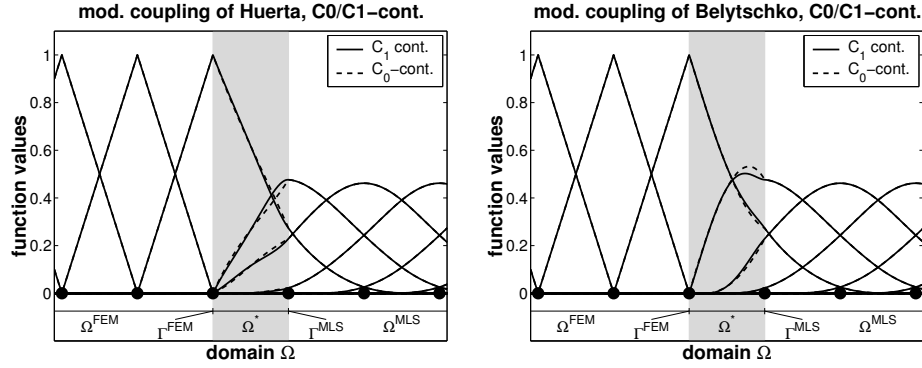


Figure 5: Comparison of C^0 and C^1 continuous shape functions along Γ^{MLS} in the modified coupling approaches.

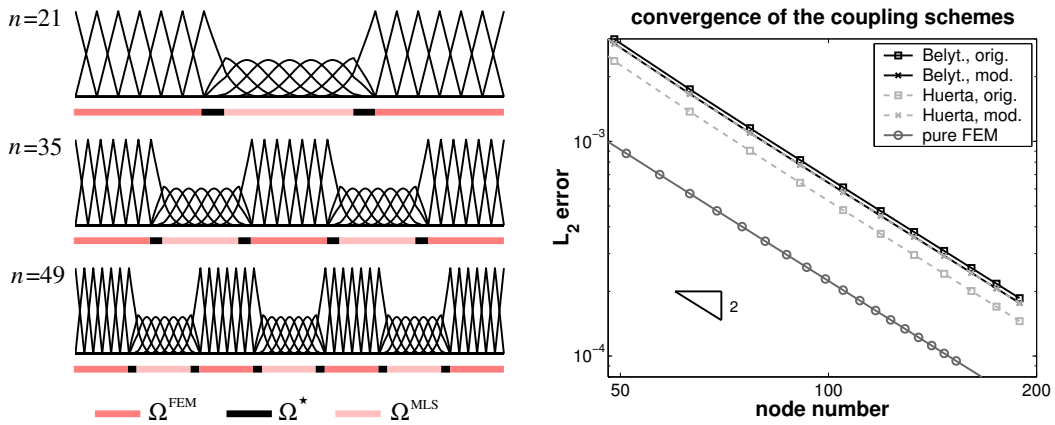


Figure 6: Convergence test of the coupling approaches.

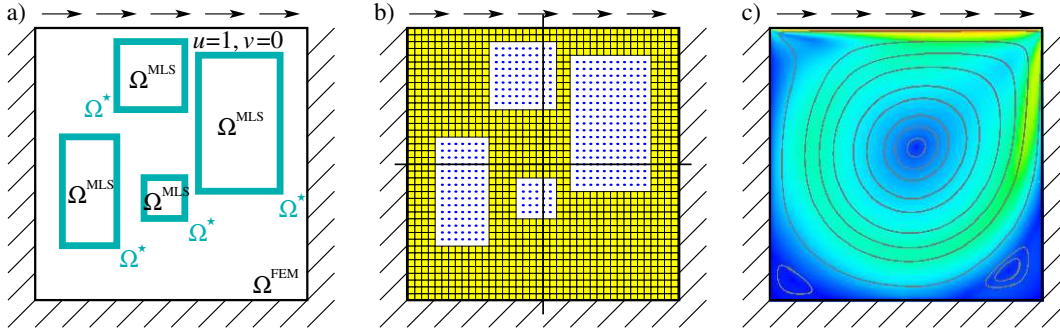


Figure 7: a) Driven cavity test case with domain decomposed into Ω^{FEM} , Ω^{MLS} and Ω^* , b) discretization with 41×41 FEM and MLS nodes, c) absolute velocity and streamlines.

to [4, 24].

5.2 Incompressible Navier-Stokes Equations

5.2.1 Driven Cavity Flow

The driven cavity test case is a standard benchmark for fluid problems. Reference solutions are given in [19]. A flow inside a quadratic domain $\Omega = (0, 1) \times (0, 1)$ with no-slip boundary conditions on the left, right and lower wall develops under a shear flow applied on the upper boundary until a stationary solution is reached. Fig. 7 gives an outline of the problem and shows a discretization with 41×41 nodes. The modified coupling approaches are applied, in order to enable the use of small dilatation parameters of $\rho_i = 1.3\Delta x$. For a Reynolds number of $\text{Re} = 1000$ convergence may not be reached for dilatation parameters $\rho_i \geq 2.0\Delta x$, underlining the importance of the modified coupling versions.

The results of both approaches are almost identical for this test case and therefore, only the result for the coupling approach in [24] is shown. Fig. 8 shows results for the unknowns u , v and p over the domain Ω ; it may be seen that the meshfree and meshbased parts fit smoothly together. In Fig. 9 the convergence against the reference solution along the vertical center velocity profile is shown, and coupled results are compared with the pure FEM solutions. The Ω^{MLS} holes are placed such that the center profile directly cuts through them. In between the MLS nodes in the figures, linear interpolation has been applied for simplicity. One may see that coupling does not adversely affect the solution.

5.2.2 Cylinder Flow

The channel flow around a cylinder has been developed as a test case e.g. in [41]. The cylinder is placed slightly unsymmetrically in y -direction of the channel. For sufficiently high Reynolds numbers, the well-known Kármán vortex street develops behind the cylinder. A quasi-stationary solution is obtained. Reference solutions are given for the lift and drag coefficients c_L and c_D of the cylinder. Fig. 10 shows a sketch of the Kármán vortex street, the discretization by FEM and MLS nodes and the development of c_D and c_L in time until a periodical solution is obtained.

In the left part of Fig. 11, the results for the drag and lift coefficient obtained with the

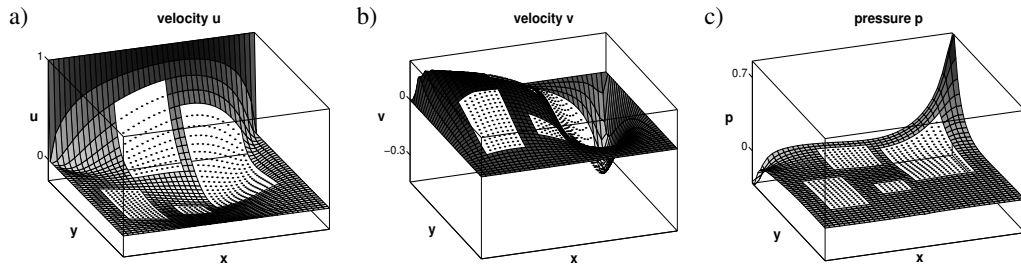


Figure 8: Solution for u , v and p over the domain Ω .

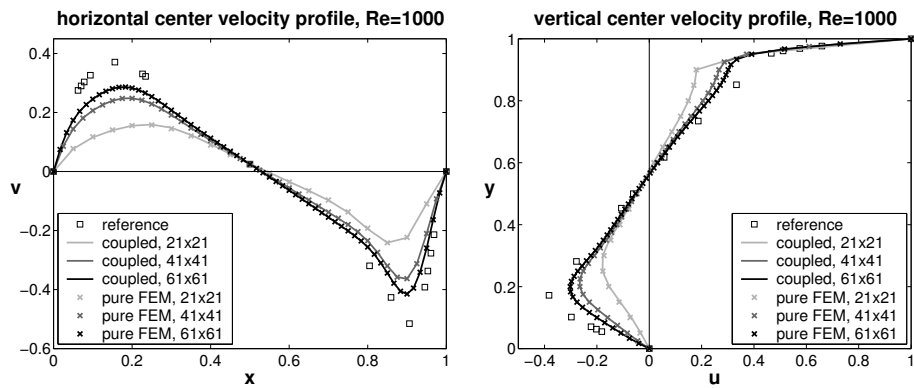


Figure 9: Velocity profiles along center cuts compare pure FEM results with the coupled results and show convergence against reference solution.

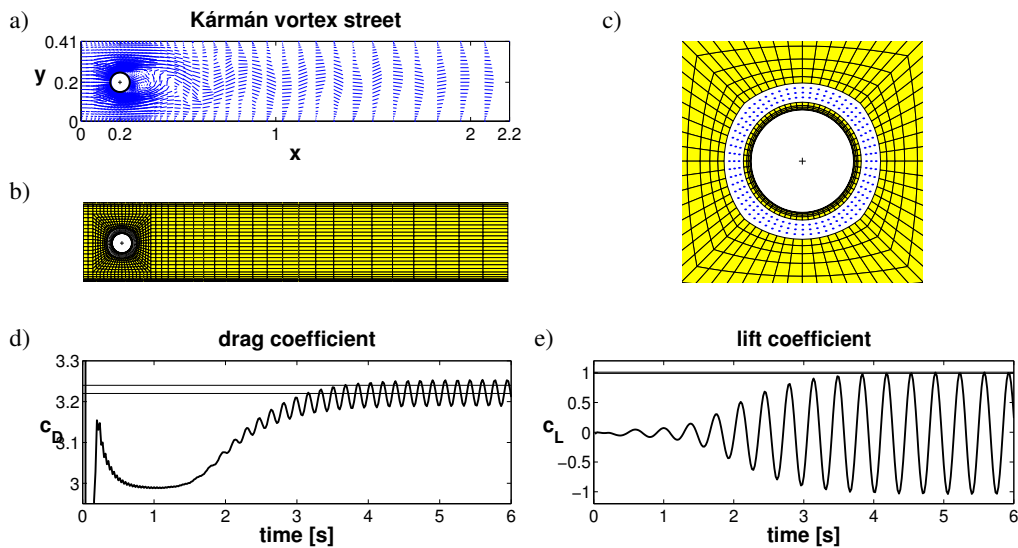


Figure 10: Cylinder test case at $Re = 100$, a) the Kármán vortex street, b) discretization of Ω , c) detail of the discretization with FEM and MLS nodes around the cylinder, d) and e) development of the drag and lift coefficient in time.

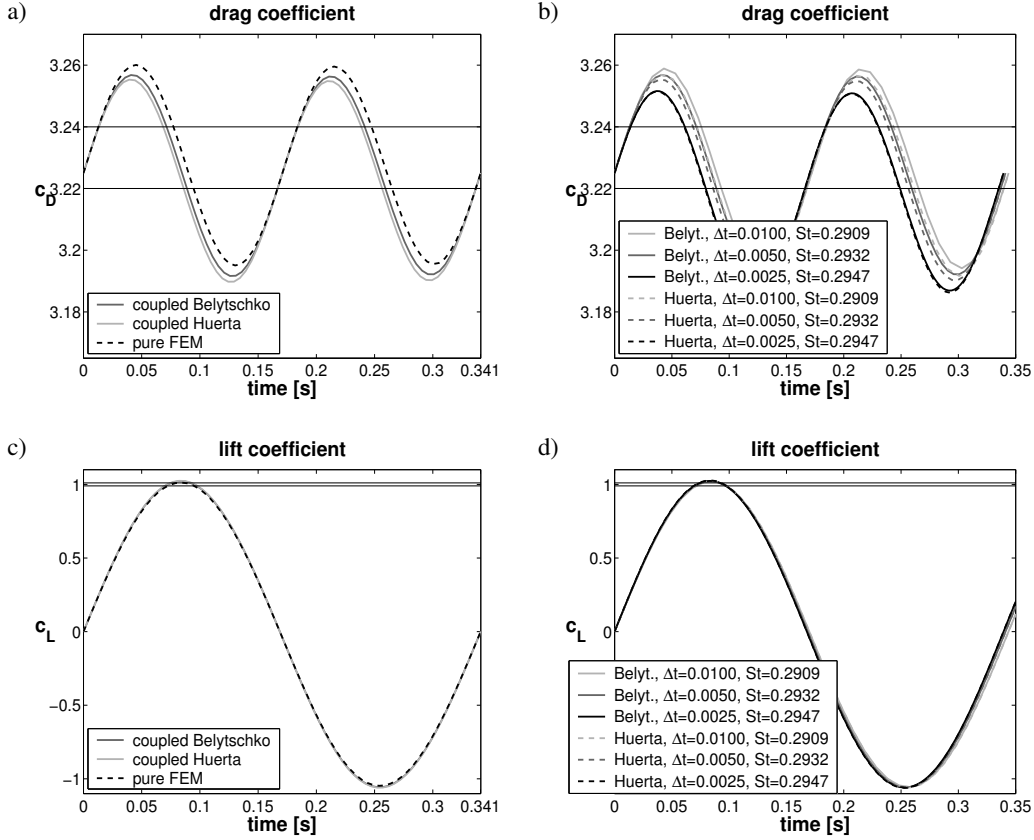


Figure 11: The left part compares the different modified coupling approaches and the pure FEM solution for $\Delta t = 0.005$, the right part shows the convergence in time of the coupled approaches.

modified approach of [4] and [24] and the pure FEM computation are compared ($\Delta t = 0.005$). The horizontal lines show the limits, in which the exact value for the maximum of c_D and c_L lie [41]. One may again see that the results are quite close together. The drag coefficient is slightly improved with the coupled approaches, the coupling approach of [24] achieves somewhat better results than the approach of [4]. Both are slightly better than the pure FEM computation. Results for the lift coefficient are almost indistinguishable, i.e. the drag coefficient turns out to be more sensitive.

The right part of Fig. 11 shows the dependence of the drag and lift coefficient on the time step Δt . The Strouhal number $St = \frac{D}{v_m T}$, with the diameter $D = 0.1$ of the cylinder, the average inflow from the left with $v_m = 1$ and the time T for 2 periods of the curve of c_D (equals 1 period of the curve of c_L), are displayed in the figure as well. A clear convergence against the reference Strouhal number of $0.295 \leq St \leq 0.305$ may be seen and the amplitudes of the drag coefficient improve.

5.2.3 Flow around a Rotating Obstacle

The previously described test cases verified the coupled fluid solver. However, they do not take advantage of the beneficial properties of this approach. The following test case replaces the cylinder

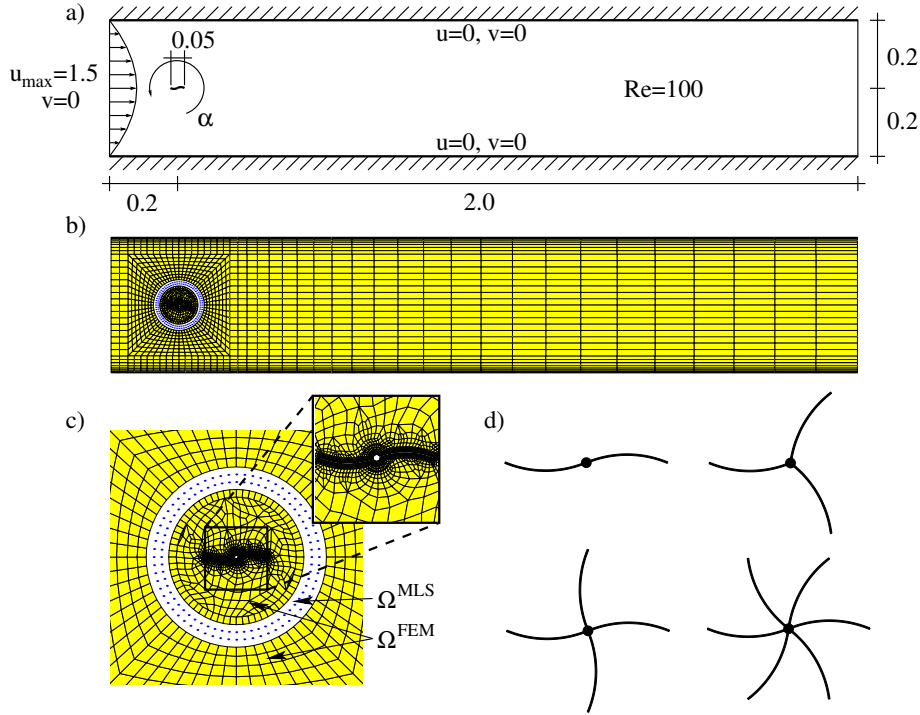


Figure 12: a) Problem statement of the rotor test case, b) and c) show the discretization and d) different rotor geometries.

of the previous test case by a rotating obstacle. A problem statement can be seen in Fig. 12a), the corresponding discretization with the meshfree and meshbased part in b) and c). One rotation is completed after 1 time unit. No-slip boundary conditions are applied on the walls and on the rotor surface, a parabolic velocity profile is prescribed at the inflow, and at the outflow traction-free boundaries are set. The coupling approach of [24] is applied as it performs somewhat better in the previous test cases.

Standard meshbased methods fail to give results due to the distortion of the mesh which must follow the rotation. However, this is no problem with the coupled fluid solver, where the rotating inner mesh and the stationary outer mesh are separated by a meshfree area. The mesh velocities of the inner mesh are considered with the arbitrary Lagrangian Eulerian (ALE) technique [27]. Fig. 13 shows vorticity results for different angles α of the two-wings rotor. In Fig. 14 the resulting momentum around the center of the rotors in dependence of the angle α of the inner mesh are shown, the geometries of the different rotors may be seen from Fig. 12d).

6 Conclusion

In the two parts of this work stabilized and coupled meshfree/meshbased methods have been established. Meshbased bi-linear finite element shape functions are coupled with meshfree moving least-squares functions. The Eulerian or ALE viewpoint has been taken for the formulation of the incompressible Navier-Stokes equations. This is standard for meshbased methods and is also used for the meshfree part to enable a straightforward coupling. Thus, stabilization is required which

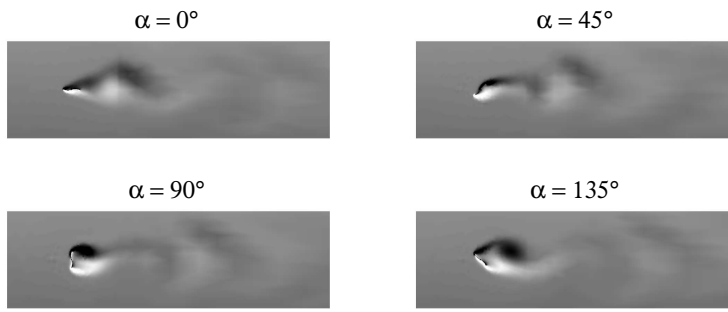


Figure 13: Vorticity for the 2-wing rotor for different angles α .

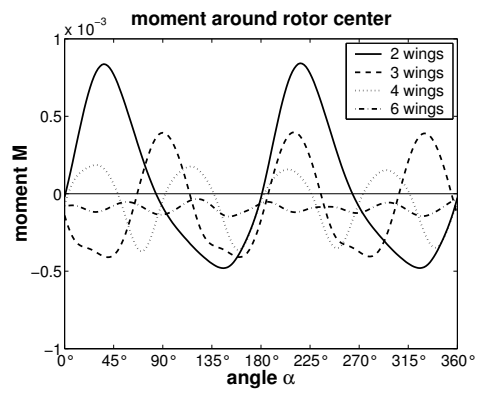


Figure 14: Resulting momentum around the center of the different rotors in dependence of the angle α .

has been discussed in part I of this work [18].

In this part different coupling ideas for meshfree and meshbased methods are reviewed. Herein, coupling is performed in order to make profit of the beneficial features of meshfree methods in complex geometry situations where conforming meshes are difficult to maintain, limiting the use of purely meshbased methods. The increased computational effort involved in using meshfree methods is minimized by coupling meshfree and meshbased shape functions, and using meshfree methods only in small parts of the domain where they are needed.

Standard coupling approaches for coupling meshfree and meshbased shape functions are described and modified such that the resulting shape functions are more suited for stabilization. This is a crucial aspect, because meshfree methods for stabilized, non-linear problems require special attention, see also [15, 17]. It is found in the numerical results that the modified coupling approach of Huerta *et al.* [24] achieves slightly better results than the approach of Belytschko *et al.* [4]. It should also be noted that using the coupling approach of Huerta *et al.* has the advantage that coupled shape functions with any desired order consistency can be obtained. Thus, higher order convergence of the coupled meshfree/meshbased simulations may be easily achieved by using higher order finite element shape functions and enriching the basis vector in the MLS procedure.

A convergence test for a one-dimensional test case shows that the coupled approaches presented herein with linear consistency achieve the same order of convergence than purely meshbased linear FEM calculations. The coupling approaches are then used for the solution of the two-dimensional incompressible Navier-Stokes equations. The coupled fluid solver is verified with standard test cases and is employed to solve a flow around a moving and rotating obstacle, showing the straightforward usability of this approach to complex flow problems.

We conclude that coupled FEM/MLS approximations are a very promising tool for the simulation of complex flow problems as they for example arise in fluid-structure-interaction problems.

References

- [1] Bakker, A.; LaRoche, R.D.; Wang, M.H.; Calabrese, R.V.: Sliding Mesh Simulation of Laminar Flow in Stirred Reactors. *Trans IChemE (Part A)*, **75**, 42 – 44, 1997.
- [2] Behr, M.; Tezduyar, T.: The Shear-Slip Mesh Update Method. *Comp. Methods Appl. Mech. Engrg.*, **174**, 261 – 274, 1999.
- [3] Belytschko, T.; Krongauz, Y.; Organ, D.; Fleming, M.; Krysl, P.: Meshless Methods: An Overview and Recent Developments. *Comp. Methods Appl. Mech. Engrg.*, **139**, 3 – 47, 1996.
- [4] Belytschko, T.; Organ, D.; Krongauz, Y.: A Coupled Finite Element–Element-free Galerkin Method. *Comput. Mech.*, **17**, 186 – 195, 1995.
- [5] Bertrand, F.; Tanguy, P.A.; Thibault, F.: A Three-dimensional Fictitious Domain Method for Incompressible Fluid Flow Problems. *Int. J. Numer. Methods Fluids*, **25**, 719 – 736, 1997.
- [6] Brooks, A.N.; Hughes, T.J.R.: Streamline upwind/Petrov-Galerkin formulations for convection dominated flows with particular emphasis on the incompressible Navier-Stokes equations. *Comp. Methods Appl. Mech. Engrg.*, **32**, 199 – 259, 1982.

- [7] Chen, T.; Raju, I.S.: Coupling finite element and meshless local Petrov-Galerkin methods for two-dimensional potential problems. AIAA 2002-1659, NASA Langley Research Center, Hampton, USA, 2002.
- [8] Chesshire, G.; Henshaw, W.D.: Composite Overlapping Meshes for the Solution of Partial Differential Equations. *J. Comput. Phys.*, **90**, 1 – 64, 1990.
- [9] Donea, J.; Huerta, A.: *Finite Element Methods for Flow Problems*. John Wiley & Sons, Chichester, 2003.
- [10] Duarte, C.A.; Oden, J.T.: An h-p adaptive method using clouds. *Comp. Methods Appl. Mech. Engrg.*, **139**, 237 – 262, 1996.
- [11] Duarte, C.A.M.; Oden, J.T.: H-p clouds – an h-p meshless method. *Numer. Methods Partial Differential Equations*, **12**, 673 – 705, 1996.
- [12] Fernández-Méndez, S.; Huerta, A.: Coupling finite elements and particles for adaptivity. In *Meshfree Methods for Partial Differential Equations*. (Griebel, M.; Schweitzer, M.A., Eds.), Vol. 26, Springer Verlag, Berlin, 2002.
- [13] Fries, T.P.; Matthies, H.G.: Classification and Overview of Meshfree Methods. Informatikbericht-Nr. 2003-03, Technical University Braunschweig, (<http://opus.tu-bs.de/opus/volltexte/2003/418/>), Brunswick, 2003.
- [14] Fries, T.P.; Matthies, H.G.: Coupled Meshfree/Meshbased Methods for Fluid Dynamics: An Alternative to the Chimera Grid Technique. *Proceedings of the XXXII International Summer School - Conference: Advanced Problems in Mechanics (APM 2004)*, St. Petersburg, Russia, 2004.
- [15] Fries, T.P.; Matthies, H.G.: A Review of Petrov-Galerkin Stabilization Approaches and an Extension to Meshfree Methods. Informatikbericht-Nr. 2004-01, Technical University of Braunschweig, (<http://opus.tu-bs.de/opus/volltexte/2004/549/>), Brunswick, 2004.
- [16] Fries, T.P.; Matthies, H.G.: Stabilized and Coupled FEM/EFM Approximations for Fluid Problems. *Proceedings of the Sixth World Congress on Computational Mechanics (WCCM VI)*, Beijing, China, 2004.
- [17] Fries, T.P.; Matthies, H.G.: Meshfree Petrov-Galerkin Methods for the Incompressible Navier-Stokes Equations. In *Meshfree Methods for Partial Differential Equations*. (Griebel, M.; Schweitzer, M.A., Eds.), Vol. 43, Springer Verlag, Berlin, 2005.
- [18] Fries, T.P.; Matthies, H.G.: A Stabilized and Coupled Meshfree/Meshbased Method for the Incompressible Navier-Stokes Equations — Part I: Stabilization. Informatikbericht-Nr. 2005-02, Technical University of Braunschweig, (<http://opus.tu-bs.de/opus/volltexte/2005/677/>), Brunswick, 2005.
- [19] Ghia, U.; Ghia, K.N.; Shin, C.T.: High-Re solutions for incompressible flow using the Navier-Stokes equations and a multi-grid method. *J. Comput. Phys.*, **48**, 387 – 411, 1982.

- [20] Glowinski, R.; Pan, T.W.; Hesla, T.I.; Joseph, D.D.; Périaux, J.: A Distributed Lagrange Multiplier/Fictitious Domain Method for Flows around Moving Rigid Bodies: Application to Particulate Flow. *Int. J. Numer. Methods Fluids*, **30**, 1043 – 1066, 1999.
- [21] Gresho, P.M.; Sani, R.L.: *Incompressible Flow and the Finite Element Method*, Vol. 1+2. John Wiley & Sons, Chichester, 2000.
- [22] Hirsch, C.: *Numerical Computation of Internal and External Flows: Fundamentals of Numerical Discretization*, Vol. 1. John Wiley & Sons, Chichester, 1988.
- [23] Houzeaux, G.; Codina, R.: A Chimera Method Based on a Dirichlet/Neumann(Robin) Coupling for the Navier-Stokes Equations. *Comp. Methods Appl. Mech. Engrg.*, **192**, 3343 – 3377, 2003.
- [24] Huerta, A.; Fernández-Méndez, S.: Enrichment and Coupling of the Finite Element and Meshless Methods. *Internat. J. Numer. Methods Engrg.*, **48**, 1615 – 1636, 2000.
- [25] Huerta, A.; Fernández-Méndez, S.M.: Time accurate consistently stabilized mesh-free methods for convection-dominated problems. *Internat. J. Numer. Methods Engrg.*, **50**, 1 – 18, 2001.
- [26] Hughes, T.J.R.: *The Finite Element Method: Linear Static and Dynamic Finite Element Analysis*. Prentice-Hall, Englewood Cliffs, NJ, 1987.
- [27] Hughes, T.J.R.; Liu, W.K.; Zimmermann, T.K.: Lagrangian-Eulerian Finite Element Formulation for Incompressible Viscous Flows. *Comp. Methods Appl. Mech. Engrg.*, **29**, 329 – 349, 1981.
- [28] Idelsohn, S.R.; Oñate, E.; Calvo, N.; Pin, F. Del: The meshless finite element method. *Internat. J. Numer. Methods Engrg.*, **58**, 893 – 912, 2003.
- [29] Johnson, G.R.; Stryk, R.A.; Beissel, S.R.: SPH for high velocity impact computations. *Comp. Methods Appl. Mech. Engrg.*, **139**, 347 – 373, 1996.
- [30] Lancaster, P.; Salkauskas, K.: Surfaces Generated by Moving Least Squares Methods. *Math. Comput.*, **37**, 141 – 158, 1981.
- [31] Li, S.; Lu, H.; Han, W.; Liu, W.K.; Simkins, D.C.: Reproducing kernel element method. Part II: Globally conforming I^m/C^n hierarchies. *Comp. Methods Appl. Mech. Engrg.*, **193**, 953 – 987, 2004.
- [32] Liu, G.R.; Gu, T.: Meshless local Petrov-Galerkin (MLPG) method in combination with finite element and boundary element approaches. *Comput. Mech.*, **26**, 536 – 546, 2000.
- [33] Liu, W.K.; Han, W.; Lu, H.; Li, S.; Cao, J.: Reproducing kernel element method. Part I: Theoretical formulation. *Comp. Methods Appl. Mech. Engrg.*, **193**, 933 – 951, 2004.
- [34] Liu, W.K.; Li, S.; Belytschko, T.: Moving Least Square Reproducing Kernel Methods (I) Methodology and Convergence. *Comp. Methods Appl. Mech. Engrg.*, **143**, 113 – 154, 1997.

- [35] Liu, W.K.; Uras, R.A.; Chen, Y.: Enrichment of the finite element method with the reproducing kernel particle method. *J. Appl. Mech., ASME*, **64**, 861 – 870, 1997.
- [36] Masud, A.; Hughes, T.J.R.: A Space-Time Galerkin/Least-Squares Finite Element Formulation of the Navier-Stokes Equations for Moving Domain Problems. *Comp. Methods Appl. Mech. Engrg.*, **146**, 91 – 126, 1997.
- [37] Melenk, J.M.; Babuška, I.: The Partition of Unity Finite Element Method: Basic Theory and Applications. *Comp. Methods Appl. Mech. Engrg.*, **139**, 289 – 314, 1996.
- [38] Mittal, S.: On the performance of high aspect ratio elements for incompressible flows. *Comp. Methods Appl. Mech. Engrg.*, **188**, 269 – 287, 2000.
- [39] Oden, J.T.; Duarte, C.A.; Zienkiewicz, O.C.: A New Cloud-based hp Finite Element Method. *Comp. Methods Appl. Mech. Engrg.*, **153**, 117 – 126, 1998.
- [40] Osher, S.; Fedkiw, R.P.: *Level Set Methods and Dynamic Implicit Surfaces*. Springer Verlag, Berlin, 2003.
- [41] Schäfer, M.; Turek, S.: Benchmark Computations of Laminar Flow around a Cylinder. In *Flow Simulation with High-Performance Computers II*. (Hirschel, E.H., Ed.), Vieweg Verlag, Braunschweig, 1996.
- [42] Shakib, F.; Hughes, T.J.R.; Johan, Z.: A new finite element formulation for computational fluid dynamics: X. The compressible Euler and Navier-Stokes equations. *Comp. Methods Appl. Mech. Engrg.*, **89**, 141 – 219, 1991.
- [43] Steger, J.L.; Benek, J.A.: On the Use of Composite Grid Schemes in Computational Aerodynamics. *Comp. Methods Appl. Mech. Engrg.*, **64**, 301 – 320, 1987.
- [44] Strouboulis, T.; Babuška, I.; Copps, K.: The design and analysis of the Generalized Finite Element Method. *Comp. Methods Appl. Mech. Engrg.*, **181**, 43 – 69, 2000.
- [45] Strouboulis, T.; Copps, K.; Babuška, I.: The Generalized Finite Element Method. *Comp. Methods Appl. Mech. Engrg.*, **190**, 4081 – 4193, 2001.
- [46] Tezduyar, T.E.: Stabilized Finite Element Formulations for Incompressible Flow Computations. In *Advances in Applied Mechanics*. (Hutchinson, J.W.; Wu, T.Y., Eds.), Vol. 28, Academic Press, New York, NY, 1992.
- [47] Turek, S.: *Efficient Solvers for Incompressible Flow Problems*, Vol. 6. Springer Verlag, Berlin, 1999.
- [48] Wagner, G.J.; Liu, W.K.: Hierarchical enrichment for bridging scales and mesh-free boundary conditions. *Internat. J. Numer. Methods Engrg.*, **50**, 507 – 524, 2001.
- [49] Wang, Z.J.; Parthasarathy, V.: A Fully Automated Chimera Methodology for Multiple Moving Body Problems. *Int. J. Numer. Methods Fluids*, **33**, 919 – 938, 2000.
- [50] Zienkiewicz, O.C.; Taylor, R.L.: *The Finite Element Method: Fluid Dynamics*, Vol. 3. Butterworth-Heinemann, Oxford, 2000.

- [51] Zienkiewicz, O.C.; Taylor, R.L.: *The Finite Element Method: Solid Mechanics*, Vol. 2. Butterworth-Heinemann, Oxford, 2000.

2000-08	T. Gehrke, U. Goltz	High-Level Sequence Charts with Data Manipulation
2000-09	T. Firley	Regular languages as states for an abstract automaton
2001-01	K. Diethers	Tool-Based Analysis of Timed Sequence Diagrams
2002-01	R. van Glabbeek, U. Goltz	Well-behaved Flow Event Structures for Parallel Composition and Action Refinement
2002-02	J. Weimar	Translations of Cellular Automata for Efficient Simulation
2002-03	H. G. Matthies, M. Meyer	Nonlinear Galerkin Methods for the Model Reduction of Nonlinear Dynamical Systems
2002-04	H. G. Matthies, J. Steindorf	Partitioned Strong Coupling Algorithms for Fluid-Structure-Interaction
2002-05	H. G. Matthies, J. Steindorf	Partitioned but Strongly Coupled Iteration Schemes for Nonlinear Fluid-Structure Interaction
2002-06	H. G. Matthies, J. Steindorf	Strong Coupling Methods
2002-07	H. Firley, U. Goltz	Property Preserving Abstraction for Software Verification
2003-01	M. Meyer, H. G. Matthies	Efficient Model Reduction in Non-linear Dynamics Using the Karhunen-Loève Expansion and Dual-Weighted-Residual Methods
2003-02	C. Täubner	Modellierung des Ethylen-Pathways mit UML-Statecharts
2003-03	T.-P. Fries, H. G. Matthies	Classification and Overview of Meshfree Methods
2003-04	A. Keese, H. G. Matthies	Fragen der numerischen Integration bei stochastischen finiten Elementen für nichtlineare Probleme
2003-05	A. Keese, H. G. Matthies	Numerical Methods and Smolyak Quadrature for Nonlinear Stochastic Partial Differential Equations
2003-06	A. Keese	A Review of Recent Developments in the Numerical Solution of Stochastic Partial Differential Equations (Stochastic Finite Elements)
2003-07	M. Meyer, H. G. Matthies	State-Space Representation of Instationary Two-Dimensional Airfoil Aerodynamics
2003-08	H. G. Matthies, A. Keese	Galerkin Methods for Linear and Nonlinear Elliptic Stochastic Partial Differential Equations
2003-09	A. Keese, H. G. Matthies	Parallel Computation of Stochastic Groundwater Flow
2003-10	M. Mutz, M. Huhn	Automated Statechart Analysis for User-defined Design Rules
2004-01	T.-P. Fries, H. G. Matthies	A Review of Petrov-Galerkin Stabilization Approaches and an Extension to Meshfree Methods
2004-02	B. Mathiak, S. Eckstein	Automatische Lernverfahren zur Analyse von biomedizinischer Literatur
2005-01	T. Klein, B. Rumpe, B. Schätz (Herausgeber)	Tagungsband des Dagstuhl-Workshop MBEES: Modellbasierte Entwicklung eingebetteter Systeme
2005-02	T.-P. Fries, H. G. Matthies	A Stabilized and Coupled Meshfree/Meshbased Method for the Incompressible Navier-Stokes Equations — Part I: Stabilization
2005-03	T.-P. Fries, H. G. Matthies	A Stabilized and Coupled Meshfree/Meshbased Method for the Incompressible Navier-Stokes Equations — Part II: Coupling